

# Applications of Geometric Algebra in Electromagnetism, Quantum Theory and Gravity

A. Lasenby, C. Doran, E. Arcaute

**ABSTRACT** We review the applications of geometric algebra in electromagnetism, gravitation and multiparticle quantum systems. We discuss a gauge theory formulation of gravity and its implementation in geometric algebra, and apply this to the fermion bound state problem in a black hole background. We show that a discrete energy spectrum arises in an analogous way to the hydrogen atom. A geometric algebra approach to multiparticle quantum systems is given in terms of the multiparticle spacetime algebra. This is applied to quantum information processing, multiparticle wave equations and to conformal geometry. The application to conformal geometry highlight some surprising links between relativistic quantum theory, twistor theory and de Sitter spaces.

**Keywords:** Geometric algebra, quantum theory, multiparticle quantum theory, conformal geometry, wave equations, Dirac equation, scattering, gauge theory, gravitation, de Sitter space, black holes, bound states.

## 1 Introduction

The applications of geometric algebra we discuss in this paper are largely to problems in relativistic physics. We start with a brief introduction to the geometric algebra of spacetime; the spacetime algebra or STA. The first application of this is to electromagnetic scattering problems. We describe a general method for solving the full Maxwell equations in the presence of an arbitrarily-shaped conductor. The second application is to the study of the Dirac equation in a black hole background. We show the existence of a spectrum of bound states created by the black hole. Each of these states has an imaginary contribution to its energy, which can be understood in terms of a decay process occurring at the singularity.

The next topic we discuss is the application of geometric algebra to conformal models of space and spacetime. The STA, for example, can also be viewed as the conformal algebra of the Euclidean plane. This pro-

vides a means of visualising Lorentz transformations which was first explored by Penrose. The conformal model of spacetime is constructed in a 6-dimensional geometric algebra. Rotors in this space encode the full spacetime conformal group and the conformal model provides a unified framework for Lorentzian, de Sitter and anti-de Sitter spaces.

The final topic we discuss is the extension of the STA approach to multiparticle quantum systems. The framework we use for this is the multiparticle spacetime algebra or MSTA. This is the geometric algebra of relativistic configuration space. It provides an ideal setting for studying problems in quantum information theory and gives a new means of encoding quantum entanglement. The MSTA is also the appropriate arena for the study of wave equations for particles with general spin. Lagrangians for multiparticle wave equations are constructed and applied to the case of a spin-0 particle, with surprising consequences for the stress-energy tensor and the coupling of the field to gravity.

On the surface, many of these topics seem quite unrelated. We hope to convince the reader that there are strong links between them, and that geometric algebra is the appropriate tool for understanding and exploiting these relationships. For example, the spacetime conformal model has a natural construction in terms of multiparticle states in the MSTA. This exposes the links between conformal geometry, the MSTA and the twistor programme. Conformal geometry and the MSTA also turn out to provide a framework for constructing supersymmetric models in geometric algebra.

The STA (spacetime algebra) is the geometric algebra of spacetime [15, 6, 7]. It is generated by four vectors  $\{\gamma_\mu\}$  which satisfy

$$\gamma_\mu \cdot \gamma_\nu = \frac{1}{2}(\gamma_\mu \gamma_\nu + \gamma_\nu \gamma_\mu) = \eta_{\mu\nu} = \text{diag}(+ - - -). \quad (1.1)$$

Throughout, Greek indices run from 0 to 3 and Latin indices run from 1 to 3. We use a signature in which  $\gamma_0^2 = -\gamma_i^2 = 1$ , and natural units  $c = \hbar = G$  are assumed throughout. The reverse operation is denoted by a tilde, as in  $\tilde{R}$ . The full STA is spanned by

$$\begin{array}{cccccc} 1 & \{\gamma_\mu\} & \{\gamma_\mu \wedge \gamma_\nu\} & \{I\gamma_\mu\} & I = \gamma_0\gamma_1\gamma_2\gamma_3 & \\ 1 \text{ scalar} & 4 \text{ vectors} & 6 \text{ bivectors} & 4 \text{ trivectors} & 1 \text{ pseudoscalar} & \end{array} \quad (1.2)$$

The algebraic properties of the STA are those of the Dirac matrices, but there is never any need to introduce an explicit matrix representation in calculations. As well as quantum theory, the STA has been applied to relativistic mechanics [16, 18, 11], scattering [7], tunnelling [13, 7], and gravitation [22]. Many of these applications are summarised in [10].

Suppose now that we wish to study physics in the rest frame defined by the  $\gamma_0$  vector. We define

$$\sigma_k = \gamma_k \gamma_0, \quad (1.3)$$

so that

$$\sigma_i \sigma_j + \sigma_j \sigma_i = 2\delta_{ij}. \quad (1.4)$$

The set  $\{\sigma_i\}$  therefore generate the geometric algebra of the three-dimensional space defined by the  $\gamma_0$  frame. We also see that

$$\sigma_1\sigma_2\sigma_3 = \gamma_1\gamma_0\gamma_2\gamma_0\gamma_3\gamma_0 = \gamma_0\gamma_1\gamma_2\gamma_3 = I, \quad (1.5)$$

so relative space and spacetime share the same pseudoscalar. The algebra of space is therefore the *even subalgebra* of the STA. This subalgebra contains the scalars and pseudoscalars, and 6 (spacetime) bivectors. These bivectors are split into timelike and spacelike bivectors by the chosen velocity vector ( $\gamma_0$  in this case). This split is conveniently illustrated by the electromagnetic bivector  $F$ . We have

$$F = \mathbf{E} + I\mathbf{B} \quad (1.6)$$

where  $\mathbf{E} = E^k\sigma_k$  is the electric field and  $\mathbf{B} = B^k\sigma_k$  the magnetic field. These are recovered from  $F$  by forming

$$\mathbf{E} = \frac{1}{2}(F - \gamma_0 F \gamma_0), \quad I\mathbf{B} = \frac{1}{2}(F + \gamma_0 F \gamma_0). \quad (1.7)$$

These expressions clearly show how the split of the (invariant) bivector  $F$  into electric and magnetic parts depends on the velocity of the observer. If  $\gamma_0$  is replaced by a different velocity, new fields are obtained.

## 2 Electromagnetism

The Maxwell equations can be written

$$\begin{aligned} \nabla \cdot \mathbf{E} &= \rho, & \nabla \cdot \mathbf{B} &= 0, \\ \nabla \wedge \mathbf{E} &= -\partial_t(I\mathbf{B}), & \nabla \wedge \mathbf{B} &= I(\mathbf{J} + \partial_t\mathbf{E}), \end{aligned} \quad (2.1)$$

where the  $\wedge$  product takes on its three-dimensional definition. If we now write  $\nabla = \gamma^\mu \partial_\mu$ ,  $J = (\rho + \mathbf{J})\gamma_0$  and  $F = \mathbf{E} + I\mathbf{B}$  the Maxwell equations combine into the single, relativistically covariant equation [15]

$$\nabla F = J. \quad (2.2)$$

Here we are interested in monochromatic scattering, which can be treated in a unified manner by introducing a free-space multivector Green's function. The essential geometry of the problem is illustrated in figure 1. The incident field  $F_i$  sets up oscillating currents in the object, which generate an outgoing radiation field  $F_s$ . The total field is given by

$$F = F_i + F_s. \quad (2.3)$$

For monochromatic waves the time dependence is conveniently expressed as

$$F(x) = F(\mathbf{r})e^{-i\omega t}, \quad (2.4)$$

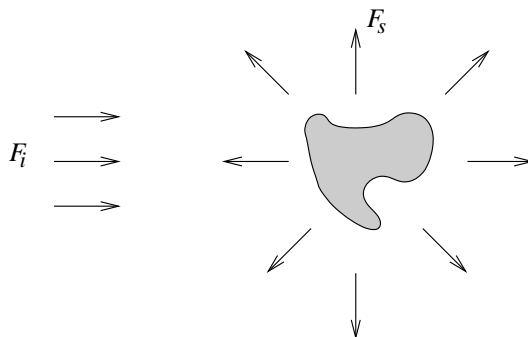


FIGURE 1. *Scattering by a localised object.* The incident field  $F_i$  sets up oscillating currents in the object, which generate an outgoing radiation field  $F_s$ .

so that the Maxwell equations reduce to

$$\nabla F - i\omega F = 0. \quad (2.5)$$

We seek a Green's function satisfying

$$\dot{G} \nabla + i\omega G = \delta(\mathbf{r}), \quad (2.6)$$

where the overdot denotes the scope of the derivative operator. The solution to this problem is

$$G(\mathbf{r}) = \frac{e^{i\omega r}}{4\pi} \left( \frac{i\omega}{r} (1 - \sigma_r) + \frac{\mathbf{r}}{r^3} \right), \quad (2.7)$$

where  $\sigma_r = \mathbf{r}/r$  is the unit vector in the direction of  $\mathbf{r}$ . If  $S_1$  denotes the surface just outside the scatterers (so that no surface currents are present over  $S_1$ ), then the scattered field can be shown to equal

$$F_s(\mathbf{r}) = \frac{1}{4\pi} \oint_{S_1} e^{i\omega d} \left( \frac{i\omega}{d} + \frac{i\omega(\mathbf{r} - \mathbf{r}')}{d^2} - \frac{\mathbf{r} - \mathbf{r}'}{d^3} \right) \mathbf{n}' F_s(\mathbf{r}') |dS(\mathbf{r}')|, \quad (2.8)$$

where

$$d = |\mathbf{r} - \mathbf{r}'|, \quad (2.9)$$

and  $\mathbf{n}$  points into the surface. The key remaining problem is to find the fields over the surface of the conductor. This is solved by treating the surface as a series of simplices and explicitly solving for the surface currents over each simplex. A subtlety here is that each part of the conductor creates a field which is seen by every other part of the conductor. The problem of finding a self-consistent solution to these equation can be converted to

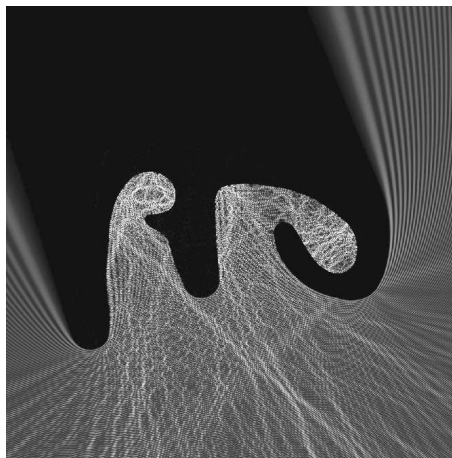


FIGURE 2. *Scattering in two dimensions.* The plots show the intensity of the electric field, with higher intensity coloured lighter.

a matrix inversion problem, which is sufficient to provide the fields over the conductor. Equation (2.8) is then an exact, analytic expression for the fields at any point in space (given the discretised model of the conductor) and the integrals can be computed numerically to any desired accuracy.

An example of this method is shown in figure 2. The calculations fully incorporate all diffraction effects and polarisations, as well as correctly accounting for obliquity factors. The plots show the intensity of the electric field, with higher intensity coloured lighter. The incident radiation enters from the bottom right of the diagram and scatters off a conductor with complicated surface features. The conductor is closed in the shadow region. Various diffraction effects are clearly visible, as is a complicated pattern of hot and cold regions.

### 3 Single-particle quantum theory and gravity

The non-relativistic wavefunction for a spin-1/2 particle is a Pauli spinor. It represents the complex superposition of two possible spin states,

$$|\psi\rangle = \alpha_1|\uparrow\rangle + \alpha_2|\downarrow\rangle, \quad (3.1)$$

where  $\alpha_1$  and  $\alpha_2$  are complex numbers. There are various means of representing  $|\psi\rangle$  in the Pauli algebra. One route is via the introduction of idempotents of the form  $\frac{1}{2}(1 + \sigma_3)$ . A more direct route, which has many advantages in computations, is to map the degrees of freedom in  $|\psi\rangle$  onto an element of the even subalgebra of the Pauli algebra [6, 21, 7]. The ap-

appropriate map is

$$|\psi\rangle = \begin{pmatrix} a^0 + ia^3 \\ -a^2 + ia^1 \end{pmatrix} \leftrightarrow \psi = a^0 + a^k I\sigma_k. \quad (3.2)$$

This map is clearly one-to-one. The spin-up and spin-down basis states are represented by

$$|\uparrow\rangle \leftrightarrow 1, \quad |\downarrow\rangle \leftrightarrow -I\sigma_2, \quad (3.3)$$

and the action of the Pauli operators on a state is represented by

$$\hat{\sigma}_k |\psi\rangle \leftrightarrow \sigma_k \psi \sigma_3 \quad (k = 1, 2, 3). \quad (3.4)$$

The factor of  $\sigma_3$  on the right-hand side of  $\psi$  ensures that  $\sigma_k \psi \sigma_3$  remains in the even subalgebra. Its presence does not break the rotational invariance because rotations are encoded in *rotors* which multiply  $\psi$  from the left.

The product of the three Pauli matrices has the same effect as the unit imaginary since

$$\hat{\sigma}_1 \hat{\sigma}_2 \hat{\sigma}_3 = \begin{pmatrix} i & 0 \\ 0 & i \end{pmatrix}. \quad (3.5)$$

It follows that

$$i|\psi\rangle \leftrightarrow \sigma_1 \sigma_2 \sigma_3 \psi (\sigma_3)^3 = \psi I\sigma_3, \quad (3.6)$$

so the action of the unit imaginary on a column spinor has been replaced by the action of a bivector.

Relativistic spin-1/2 states are described by Dirac spinors. These have 8 real degrees of freedom and can be represented by the even subalgebra of the full STA. The corresponding action of the Dirac matrices and the unit imaginary is then

$$\hat{\gamma}_\mu |\psi\rangle \leftrightarrow \gamma_\mu \psi \gamma_0 \quad (\mu = 0, \dots, 3) \quad (3.7)$$

$$i|\psi\rangle \leftrightarrow \psi I\sigma_3. \quad (3.8)$$

In this representation, the Dirac equation takes the form [15, 6, 7]

$$\nabla \psi I\sigma_3 - eA\psi = m\psi\gamma_0 \quad (3.9)$$

where  $A = \gamma^\mu A_\mu$ .

We will shortly examine this equation in a gravitational context.

### 3.1 Gravity as a gauge theory

Gravity was first formulated as a gauge theory in the 1960s by Kibble [19]. It turns out that this approach to gravity allows us to develop a theory which fully exploits the advantages of the STA [22]. The theory is constructed in terms of gauge fields in a flat spacetime background. Features of the background space are not gauge invariant, so are not physically measurable.

This is the manner in which the gauge theory approach frees us from any notion of an absolute space or time. The theory requires two gauge fields; one for local translations and one for Lorentz transformations. The first of these can be understood by introducing a set of coordinates  $x^\mu$ , with associated coordinate frame  $e_\mu$ . In terms of these we have

$$\nabla = e^\mu \partial_\mu, \quad (3.10)$$

and the Lorentzian metric is

$$ds^2 = e_\mu \cdot e_\nu dx^\mu dx^\nu. \quad (3.11)$$

The gauging step is now simply to replace the  $e_\mu$  frame with a set of gauge fields  $g_\mu$  which are no longer tied to a flat-space coordinate frame. That is, we take

$$e_\mu(x) \mapsto g_\mu(x). \quad (3.12)$$

This requires the introduction of 16 gauge degrees of freedom for the four vectors  $g_\mu$ . The gauge-invariant line element is now

$$ds^2 = g_\mu \cdot g_\nu dx^\mu dx^\nu, \quad (3.13)$$

from which we can read off that the effective metric is given by

$$g_{\mu\nu} = g_\mu \cdot g_\nu. \quad (3.14)$$

It is possible to develop general relativity in terms of the  $g_\mu$  alone, since these vectors are sufficient to recover a metric. But quantum theory requires a second gauge field associated with Lorentz transformations (a spin connection), and the entire theoretical framework is considerably simpler if this is included from the start. The connection consists of a set of four bivector fields  $\Omega_\mu$ , which contain 24 degrees of freedom. The full gauge theory is then a first-order theory with 40 degrees of freedom. This is usually easier to work with than the second-order metric theory (with 10 degrees of freedom) because the first-order equations afford better control over the non-linearities in the theory. The final theory is locally equivalent to the Einstein–Cartan–Kibble–Sciama (ECKS) extension of general relativity. But the fact that the gauge theory is constructed on a topologically trivial flat spacetime can have physical consequences, even if these are currently mainly restricted to theoretical discussions.

The minimally-coupled Dirac equation is defined by

$$g^\mu D_\mu \psi I\sigma_3 = m\psi\gamma_0, \quad (3.15)$$

where

$$D_\mu \psi = \left( \partial_\mu + \frac{1}{2} \Omega_\mu \right) \psi. \quad (3.16)$$

A consequence of minimal coupling is that, if we form the classical point-particle limit of the Dirac theory, we find that the mass term drops out

of the effective equation of motion. So classical particles follow trajectories (geodesics) that do not depend on their mass. This form of the equivalence principle follows directly from minimal coupling in the gauge-theory context.

### 3.2 Schwarzschild black holes

The Schwarzschild solution, written in terms of the time measured by observers in radial free-fall from rest at infinity, is given by [9]

$$ds^2 = dt^2 - \left( dr + \left( \frac{2GM}{r} \right)^{1/2} dt \right)^2 - r^2 d\Omega^2. \quad (3.17)$$

If we let  $\{e_r, e_\theta, e_\phi\}$  denote a standard spatial polar-coordinate frame, we can set

$$g_0 = \gamma_0 + \left( \frac{2GM}{r} \right)^{1/2} e_r, \quad g_i = \gamma_i, \quad (i = r, \theta, \phi). \quad (3.18)$$

The  $g_\mu$  vectors are easily shown to reproduce the metric of equation (3.17). The Dirac equation in a black-hole background, with the present gauge choices, takes the simple form [9]

$$\nabla\psi I\sigma_3 - \left( \frac{2GM}{r} \right)^{1/2} \gamma_0 \left( \partial_r\psi + \frac{3}{4r}\psi \right) I\sigma_3 = m\psi\gamma_0. \quad (3.19)$$

The full, relativistic wave equation for a fermion in a spherically-symmetric black hole background reduces to the free-field equation with a single interaction term  $H_I$ , where

$$H_I\psi = \left( \frac{2GM}{r} \right)^{1/2} i\hbar \left( \partial_r\psi + \frac{3}{4r}\psi \right). \quad (3.20)$$

(Here we have inserted dimensional constants for clarity.) Our choice of gauge has converted the problem to a Hamiltonian form, though with a non-Hermitian interaction Hamiltonian, which satisfies

$$H_I - H_I^\dagger = -i\hbar(2GMr^3)^{1/2}\delta(\mathbf{x}). \quad (3.21)$$

This gauge provides a number of insights for quantum theory in black hole backgrounds. It has recently been used to compute the fermion scattering cross section, providing the gravitational analogue of the Mott formula [9], and also applied to the bound state problem [27].

A gravitational bound state is a state with separable time dependence and which is spatially normalizable. These states form a discrete spectrum

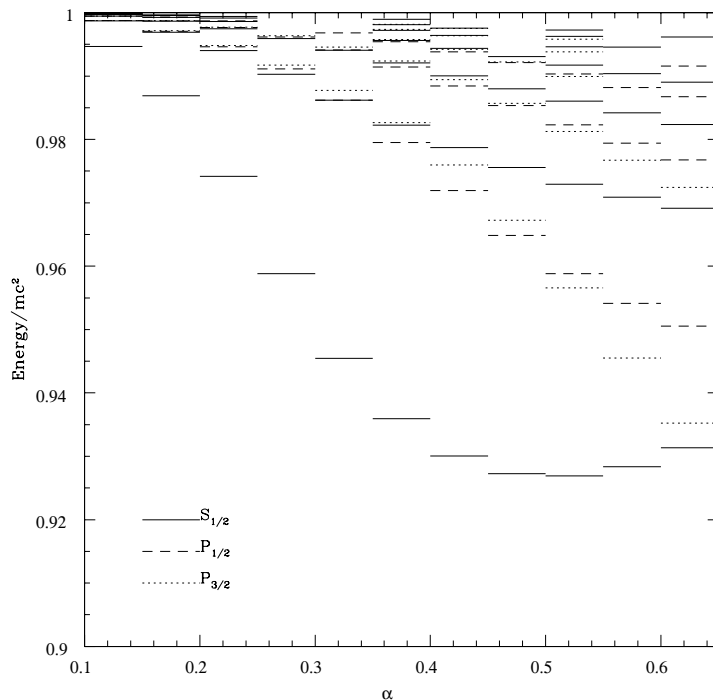


FIGURE 3. The real part of the bound state energy, in units of  $mc^2$ . The lines represent the value of the energy for the coupling at the left of the line, with  $\alpha$  ranging from 0.1 to 0.6 in steps of 0.05.

in an analogous manner to the Hydrogen atom. But the lack of Hermiticity of  $H_I$  implies that the energies also contain an imaginary component, which ensures that the states *decay*. A discrete spectrum is a consequence of the fact that boundary conditions must be simultaneously applied at the horizon and at infinity. For a given complex energy we can simultaneously integrate in from infinity and out from the horizon. These integrated functions will in general not match and so fail to generate a solution. Matching only occurs at specific discrete energy eigenvalues, distributed over the complex plane.

A sample energy spectrum is shown in figure 3, which plots the real part of the energy, in units of  $mc^2$ , for the  $S_{1/2}$ ,  $P_{1/2}$  and  $P_{3/2}$  states. (We follow the standard spectroscopic naming conventions.) The plots are shown as a function of the dimensionless coupling constant  $\alpha$ ,

$$\alpha = \frac{mM}{m_p^2}, \quad (3.22)$$

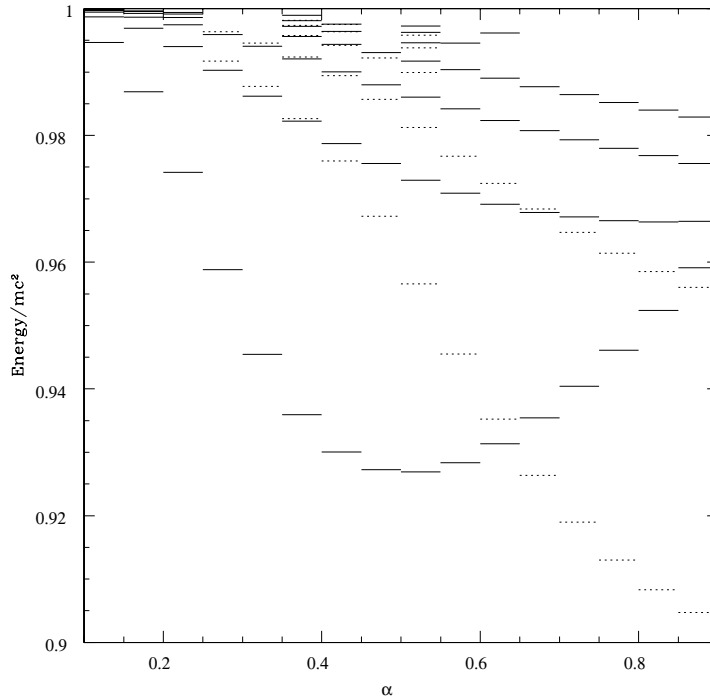


FIGURE 4. The energy spectra of the  $S_{1/2}$  (solid) and  $2P_{3/2}$  (dashed) states. Beyond a coupling of around  $\alpha = 0.65$  the  $2P_{3/2}$  state takes over as the system's ground state.

where  $m_p$  is the Planck mass. For  $m$  the mass of an electron and  $\alpha \approx 1$  then  $M$  is in the range appropriate for primordial black holes. The plots need to be extended to much larger values of  $\alpha$  to describe solar mass black holes. One feature of the real part of the energy is seen more clearly in figure 4. Beyond a coupling of around  $\alpha = 0.65$  the  $1S_{1/2}$  is no longer the system ground state, which passes to the  $2P_{3/2}$  state. This corresponds to the classical observation that the lowest energy stable circular orbits around a black hole have increasing angular momentum for increasing black hole mass.

A substantial amount of work remains in this area. The spectrum needs to be computed for much larger values of  $\alpha$ , and the work also needs to be extended to the Kerr and Reissner–Nordstrom cases. For each eigenstate the real energy is accompanied by a decay rate, which shows that the wavefunction evolution is not unitary. This is essentially because the black hole acts as an open system. One would therefore like to understand the decay rates in terms of a more complete, quantum description of a singularity. So

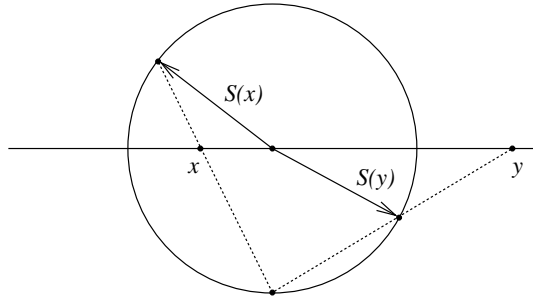


FIGURE 5. *The stereographic projection.* Given a point  $x$  we form the line through this point and the south pole of the sphere. The point where this line intersects the sphere defines the image of the projection.

far such a description has proved elusive. Furthermore, a fundamental question to address is whether the energy differences between shells corresponds to anything observable. Can quantum states spontaneously jump to lower orbits, with associated radiation? This behaviour is to be expected from the analogy with the Hydrogen atom, but is rather different to the classical picture of stable orbits around a black hole. Finally, we would clearly like to incorporate multiparticle effects in the description of the quantum physics around a black hole. Some ideas in this direction are discussed in section 5.

## 4 Conformal geometry

Conformal models of Euclidean geometry are currently the source of much interest in the computer graphics community [8]. Here we aim to illustrate some features of spacetime conformal geometry. A useful starting point for constructing conformal models is the stereographic projection (figure 5). We start with a Euclidean base space  $\mathbb{R}^n$  of dimension  $n$ , and label points in this space with vectors  $x$  from some chosen origin. The stereographic projection maps the entire space  $\mathbb{R}^n$  onto the unit sphere in  $\mathbb{R}^{n+1}$ . If we let  $e$  denote the (new) vector perpendicular to the Euclidean base space, pointing to the South pole of the sphere, then the image on the sphere of the point  $x$  is

$$S(x) = \cos \theta \hat{x} - \sin \theta e, \quad (4.1)$$

where  $\theta$  is obtained from the distance  $r = |x|$  by

$$\cos \theta = \frac{2r}{1+r^2}, \quad \sin \theta = \frac{1-r^2}{1+r^2}. \quad (4.2)$$

The stereographic projection has two important features. This first is that the origin of  $\mathbb{R}^n$  is mapped to  $-e$  and so is no longer a special point. That is, it is no longer represented by the zero vector. The second is that the point at infinity is mapped to  $e$ , so is also no longer algebraically special. Both of these features are valuable in graphics applications. Most computer graphics routines, including OpenGL, employ a projective representation of  $\mathbb{R}^n$ , as opposed to a stereographic one. The projective representation has the further advantage that it is *homogeneous*. In a homogeneous representation both  $X$  and  $\lambda X$  represent the *same* point in  $\mathbb{R}^n$ , even if  $\lambda$  is *negative*. Such a representation is crucial if one wishes to let blades represent geometric objects. If  $B$  denotes a blade, then the geometric object associated with  $B$  is the solution space of the equation

$$B \wedge X = 0. \quad (4.3)$$

Clearly, if  $X$  solves this equation, then so does  $\lambda X$ .

To convert the result of the stereographic projection to a homogeneous representation we introduce a further vector  $\bar{e}$  with negative norm,  $\bar{e}^2 = -1$ . We now add this to the result of the stereographic projection to form the vector

$$X = S(x) + \bar{e}. \quad (4.4)$$

This vector is now *null*,  $X^2 = 0$ . This condition is homogeneous, so we can let  $X$  and  $\lambda X$  represent the same Euclidean point  $x$ . Two important null vectors are provided by

$$n = e + \bar{e}, \quad \bar{n} = e - \bar{e}, \quad (4.5)$$

which represent the point at infinity ( $n$ ) and the origin ( $\bar{n}$ ). With a rescaling, we can now write the map from the Euclidean point  $x$  to a null vector  $X$  as

$$X = F(x) = -(x - e)n(x - e) = (x^2n + 2x - \bar{n}). \quad (4.6)$$

This clearly results in a null vector,  $X^2 = 0$ , as it is formed by a reflection of  $n$ . Of course,  $X$  can be arbitrarily rescaled and still represent the same point, but the representation in terms of  $F(x)$  is often convenient in calculations.

#### 4.1 Euclidean transformations

If we form the inner product of two conformal vectors, we find that

$$F(x) \cdot F(y) = -2|x - y|^2. \quad (4.7)$$

So conformal geometry encodes distances in a natural way [12, 17]. This is its great advantage over projective geometry as a framework for Euclidean space. Allowing for arbitrary scaling we have

$$|x - y|^2 = -2 \frac{X \cdot Y}{X \cdot n Y \cdot n}, \quad (4.8)$$

which is manifestly homogeneous in  $X$  and  $Y$ . This formula returns the dimensionless distance. To introduce dimensions we require a fundamental length scale  $\lambda$ , so that we can then write

$$F(x) = \frac{1}{\lambda^2}(x^2n + 2\lambda x - \lambda^2\bar{n}). \quad (4.9)$$

This is simply the conformal representation of  $x/\lambda$ .

The group of Euclidean transformations consists of all transformations of Euclidean space which leave distances invariant. In conformal space these must leave the inner product invariant, so are given by reflections and rotations. Since the South pole represents the point at infinity, we expect that any Euclidean transformation of the base space will leave the  $n$  unchanged. This requirement is also clear from equation (4.8). For example, rotations about the origin in  $\mathbb{R}^n$  are given by

$$x \mapsto Rx\tilde{R}, \quad (4.10)$$

where  $R$  is a rotor. The image of the transformed point is

$$F(Rx\tilde{R}) = x^2n + 2Rx\tilde{R} - \bar{n} = R(x^2n + 2x - \bar{n})\tilde{R} = RX\tilde{R}, \quad (4.11)$$

which follows since  $Rn\tilde{R} = n$  and  $R\bar{n}\tilde{R} = \bar{n}$ . Rotations about the origin are therefore given by the same formula in both spaces. Of greater interest are *translations*. We define the rotor  $T_a$  by

$$T_a = e^{na/2} = 1 + \frac{na}{2}. \quad (4.12)$$

This satisfies

$$\begin{aligned} T_a X \tilde{T}_a &= \frac{1}{2} \left(1 + \frac{na}{2}\right) (x^2n + 2x - \bar{n}) \left(1 - \frac{na}{2}\right) \\ &= \frac{1}{2} \left( (x+a)^2n + 2(x+a) - \bar{n} \right) \\ &= F(x+a). \end{aligned} \quad (4.13)$$

So the conformal rotor  $T_a$  performs a translation in Euclidean space. (This is the origin of the biquaternion approach in three dimensions.) Furthermore, since translations and rotations about the origin are handled by rotors, it is possible to construct simple rotors encoding rotations about arbitrary points. Such operations are essential in graphics routines.

## 4.2 Minkowski and de Sitter spaces

The conformal framework applies straightforwardly to spacetime. One immediate observation is that spacetime can be viewed as a conformal model for the plane. This provides a method of visualising the Lorentz group in terms of conformal (angle-preserving) transformations of the plane, or

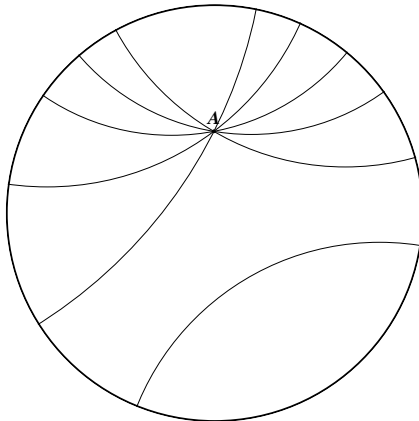


FIGURE 6. *The Poincaré disc.* Points inside the disc represent points in a hyperbolic space. A set of  $d$ -lines are also shown.

the 2-sphere. This model has been developed extensively by Penrose & Rindler [31]. Of greater interest here is the conformal model of full spacetime. In this model points in spacetime are described by null vectors in a space of signature  $(2, 4)$ . The conformal representation is again constructed by equation (4.6), with  $x = x^\mu \gamma_\mu$  a point in spacetime.

In conformal geometry, lines and circles are treated in a unified manner as trivector blades. That is, the unique line through  $A$ ,  $B$  and  $C$  is encoded by the trivector  $L = A \wedge B \wedge C$ . If  $L$  includes the point at infinity, the line is straight. A circle is the set of all points in a plane a fixed distance from some chosen point (if the line is straight the ‘centre’ is at infinity). Circles in Lorentzian spaces therefore include hyperbolas with lightlike asymptotes. So trivector blades in the geometric algebra  $\mathcal{G}(2, 4)$  can define straight lines, circles and (both branches of a) hyperbola in a single unified manner. A straightforward example of a hyperbola is the trivector  $\gamma_0 \gamma_1 \bar{e}$ . This encodes the set of all points in the  $\gamma_0 \gamma_1$  plane satisfying  $x^2 = 1$ .

A significant feature of the conformal picture is that it easily generalises to include hyperbolic and spherical geometry [28, 25, 10]. To convert from a conformal model of Euclidean space to spherical space we simply replace the distance formula of equation (4.8) by

$$d(x, y) = 2\lambda \sin^{-1} \left( -\frac{X \cdot Y}{2X \cdot \bar{e} Y \cdot \bar{e}} \right)^{1/2}, \quad (4.14)$$

so  $\bar{e}$  replaces  $n$  to convert to spherical geometry. All conformal representations of objects (points, lines etc.) are unchanged, though their geometric interpretation is altered. Similarly, hyperbolic geometry is recovered by

imposing the distance measure

$$d(x, y) = 2\lambda \sinh^{-1} \left( -\frac{X \cdot Y}{2X \cdot e Y \cdot e} \right)^{1/2}. \quad (4.15)$$

The straight line, or geodesic, through two points  $X$  and  $Y$  in a hyperbolic geometry is defined by the trivector  $X \wedge Y \wedge e$ . These are called  $d$ -lines in two dimensions. If we plot hyperbolic points on the Euclidean plane we arrive at the Poincaré disk model of two-dimensional hyperbolic geometry (figure 6). In this picture  $d$ -lines are (Euclidean) circles which intersect the unit circle at right angles. Figure 6 illustrates the hyperbolic version of the parallel postulate. Given a line, and a point  $A$  not on the line, one can construct infinitely many lines through  $A$  which do not intersect the original line. (For Euclidean geometry only one line exists, and there are none for spherical geometry).

Similar considerations apply to the accompanying symmetry groups. The Euclidean group is the set of conformal reflections and rotations which leave  $n$  invariant. Similarly, spherical transformations keep  $\bar{e}$  invariant and hyperbolic transformations keep  $e$  invariant. A natural question, then, is how does this generalise to spacetime. The answer is quite straightforward. The geometry obtained by keeping  $e$  invariant is that of de Sitter space, and for  $\bar{e}$  we recover anti-de Sitter space (AdS). The second of these is currently the subject of much interest due to the AdS/CFT correspondence and its relation to the holographic principle [29]. It is therefore gratifying to see that anti-de Sitter space has a very natural encoding in geometric algebra. For example, the geodesic through the points with conformal representation  $X$  and  $Y$  is encoded in the trivector  $X \wedge Y \wedge \bar{e}$ , see [20]. These lines can be intersected, reflected, etc. in an extremely straightforward manner. The same operations are considerably harder to formulate if one adopts the tools of differential geometry.

## 5 Multiparticle quantum theory

The STA representation of single-particle quantum states has existed since the 1960s. But it was only in the 1990s that this approach was successfully generalised to multiparticle systems [7]. The essential construction is the geometric algebra of the  $4n$ -dimensional relativistic configuration space. This is called the multiparticle spacetime algebra or MSTA. With a separate copy of spacetime for each particle present, the MSTA is generated by the  $4n$  vectors  $\{\gamma_\mu^a\}$ ,  $\mu = 0, \dots, 3$ ,  $a = 1, \dots, n$ . These satisfy

$$\gamma_\mu^a \cdot \gamma_\nu^b = \frac{1}{2}(\gamma_\mu^a \gamma_\nu^b + \gamma_\nu^b \gamma_\mu^a) = \eta_{\mu\nu} \delta^{ab}, \quad (5.1)$$

so generators from distinct spaces all anticommute.

Relative bivectors from separate spaces are constructed in the same way as the single-particle case. Again taking  $\gamma_0^a$  to represent the frame velocity vector, we write

$$\sigma_k^a = \gamma_k^a \gamma_0^a. \quad (5.2)$$

But now we see that for  $a \neq b$  the bivectors from different spaces *commute*

$$\sigma_i^a \sigma_j^b = \gamma_i^a \gamma_0^a \gamma_j^b \gamma_0^b = \gamma_i^a \gamma_j^b \gamma_0^b \gamma_0^a = \gamma_j^b \gamma_0^b \gamma_i^a \gamma_0^a = \sigma_j^b \sigma_i^a. \quad (5.3)$$

This provides a natural construction of the tensor product in terms of the geometric product. As such, the MSTA is clearly a natural arena to study multiparticle Hilbert space, which itself is constructed from a tensor product of the individual Hilbert spaces.

The simplest construction of a 2-particle state in the MSTA is as the product of two single particle spinors,  $\phi^1 \psi^2$ . But this generates a space of 64 real dimensions, whereas we only expect 32 (for the 16-dimensional complex space). We have failed to account for the fact that quantum theory requires a single, global complex structure. We must therefore ensure that post-multiplying the states by either  $(I\sigma_3)^1$  or  $(I\sigma_3)^2$  results in the same state. That is

$$\psi(I\sigma_3)^1 = \psi(I\sigma_3)^2. \quad (5.4)$$

A simple rearrangement now yields

$$\psi = -\psi(I\sigma_3)^1(I\sigma_3)^2 = \psi \frac{1}{2}(1 - (I\sigma_3)^1(I\sigma_3)^2) \quad (5.5)$$

If we now define

$$E = \frac{1}{2}(1 - (I\sigma_3)^1(I\sigma_3)^2), \quad (5.6)$$

we see that all states must satisfy

$$\psi = \psi E. \quad (5.7)$$

The 2-particle *correlator*  $E$  is an idempotent,  $E^2 = E$ , and so it removes precisely half the degrees of freedom from a general product state, as required. The complex structure is now provided by right multiplication by the multivector  $J$ , where

$$J = E(I\sigma_3)^1 = E(I\sigma_3)^2 = \frac{1}{2}((I\sigma_3)^1 + (I\sigma_3)^2). \quad (5.8)$$

It follows that  $J^2 = -E$ .

## 5.1 Entanglement

Entanglement is perhaps the key feature of the quantum world without a classical counterpart. Entangled (pure) states are those which cannot be

factored into a direct product of single-particle states. A simple example is provided by the non-relativistic singlet state

$$|\chi\rangle = \frac{1}{\sqrt{2}} \left\{ \begin{pmatrix} 1 \\ 0 \end{pmatrix} \otimes \begin{pmatrix} 0 \\ 1 \end{pmatrix} - \begin{pmatrix} 0 \\ 1 \end{pmatrix} \otimes \begin{pmatrix} 1 \\ 0 \end{pmatrix} \right\}. \quad (5.9)$$

The MSTA version of this is

$$\chi = \frac{1}{\sqrt{2}} ((I\sigma_2)^1 - (I\sigma_2)^2)E. \quad (5.10)$$

This satisfies the following property:

$$(I\sigma_k)^1\chi = -(I\sigma_k)^2\chi, \quad k = 1 \dots 3. \quad (5.11)$$

So if  $M$  is a multivector of the form  $M = M^0 + M^k I\sigma_k$ , we have

$$M^1\chi = \tilde{M}^2\chi. \quad (5.12)$$

This provides a quick proof that the singlet state is rotationally invariant, since under a joint rotation

$$\chi \mapsto R^1 R^2 \chi = R^1 \tilde{R}^1 \chi = \chi, \quad (5.13)$$

where  $R$  is a spatial rotor.

A useful parameterisation of a general 2-particle state is provided by the Schmidt decomposition, which enables us to write a non-relativistic state as

$$\begin{aligned} |\psi\rangle &= \cos(\eta/2)e^{i\tau/2} \begin{pmatrix} \cos(\phi^1/2)e^{i\theta^1/2} \\ \sin(\phi^1/2)e^{-i\theta^1/2} \end{pmatrix} \otimes \begin{pmatrix} \cos(\phi^2/2)e^{i\theta^2/2} \\ \sin(\phi^2/2)e^{-i\theta^2/2} \end{pmatrix} \\ &+ \sin(\eta/2)e^{-i\tau/2} \begin{pmatrix} \sin(\phi^1/2)e^{-i\theta^1/2} \\ -\cos(\phi^1/2)e^{i\theta^1/2} \end{pmatrix} \otimes \begin{pmatrix} \sin(\phi^2/2)e^{-i\theta^2/2} \\ -\cos(\phi^2/2)e^{i\theta^2/2} \end{pmatrix}. \end{aligned} \quad (5.14)$$

The MSTA version of the Schmidt decomposition is very revealing. We let

$$\begin{aligned} R &= \exp(\theta^1 I\sigma_3/2) \exp(-\phi^1 I\sigma_2/2) \exp(\tau I\sigma_3/2) \\ S &= \exp(\theta^2 I\sigma_3/2) \exp(-\phi^2 I\sigma_2/2) \exp(\tau I\sigma_3/2) \end{aligned} \quad (5.15)$$

so that we can write

$$\psi = R^1 S^2 (\cos(\eta/2) + \sin(\eta/2)(I\sigma_2)^1 (I\sigma_2)^2)E. \quad (5.16)$$

This neat expression shows how all information regarding the entanglement is contained in a single term on the right of the product state. This gives a form of decomposition which generalises to arbitrary numbers of particles, though the calculations are far from straightforward and much work remains [30]. Geometric algebra brings geometric insight into the nature of the multiparticle Hilbert space and can be used to quantify the nature of entanglement for pure and mixed states. This approach has helped develop new models of decoherence, some of which are currently being tested in nuclear magnetic resonance experiments [14].

## 5.2 Relativistic states and wave equations

We now turn to relativistic multiparticle states. There are many theoretical problems encountered in constructing a wavefunction treatment of interacting particles and we will not discuss these issues here. (See Dolby & Gull for a recent [4] account of the case of non-interacting particles in a classical background electromagnetic field.) Here we wish to demonstrate how the MSTA is used for constructing wave equations for particles with spin other than 1/2. This adapts the work of Bargmann & Wigner [2].

We start with a 2-particle relativistic wavefunction, which is a function of the four spacetime coordinates  $x^\mu$ , so

$$\psi = \psi(x^\mu)E. \quad (5.17)$$

This satisfies the 2-particle Dirac equation of the form

$$\nabla^1 \psi^1 J \gamma_0^1 = m \psi. \quad (5.18)$$

Any dependence on the particle space label is removed by assigning definite symmetry or antisymmetry to  $\psi$  under particle interchange. A spin-1 equation is constructed from a symmetric  $\psi$ , and a spin-0 equation from an antisymmetric  $\psi$ . It is the latter that interests us here. To simplify this problem we first introduce the relativistic singlet states

$$\begin{aligned} \epsilon &= ((I\sigma_2)^1 - (I\sigma_2)^2) \frac{1}{2}(1 + \sigma_3^1) \frac{1}{2}(1 + \sigma_3^2) E, \\ \bar{\epsilon} &= ((I\sigma_2)^1 - (I\sigma_2)^2) \frac{1}{2}(1 - \sigma_3^1) \frac{1}{2}(1 - \sigma_3^2) E. \end{aligned} \quad (5.19)$$

These are both relativistic states because they contain factors of the idempotent  $\frac{1}{2}(1 - I^1 I^2)$ . This is sufficient to ensure that, for a general even multivector  $M$ , we have

$$M^1 \epsilon = \tilde{M}^2 \epsilon, \quad M^1 \bar{\epsilon} = \tilde{M}^2 \bar{\epsilon}. \quad (5.20)$$

In particular, if  $R$  is a relativistic rotor and we perform a joint Lorentz transformation in both spaces, we see that

$$\epsilon \mapsto R^1 R^2 \epsilon = R^1 \tilde{R}^1 \epsilon = \epsilon, \quad (5.21)$$

with the same property holding for  $\bar{\epsilon}$ . The 32 real degrees of freedom in an arbitrary relativistic 2-particle state can be mapped into particle-1 space by writing

$$\psi = M^1 \epsilon + N^1 \bar{\epsilon} + s^1 \epsilon \gamma_0^1 + t^1 \bar{\epsilon} \gamma_0^1, \quad (5.22)$$

where  $M$  and  $N$  are general even-grade multivectors, and  $s$  and  $t$  are odd-grade.

As  $\epsilon$  and  $\bar{\epsilon}$  are antisymmetric under particle interchange, an antisymmetric state must have  $M = \tilde{M}$ ,  $N = \tilde{N}$  and  $\tilde{t} = s$ . The twelve scalar

degrees of freedom in a general antisymmetric wavefunction can therefore be written as

$$\psi = (\alpha + I^1\beta)\epsilon + (\theta + I^1\eta)\bar{\epsilon} + (u + Iv)^1\bar{\epsilon}J\gamma_0^1 + (u - Iv)^1\epsilon J\gamma_0^1, \quad (5.23)$$

where  $u$  and  $v$  are vectors, and  $\alpha$ ,  $\beta$ ,  $\theta$ ,  $\eta$  are scalars. A joint rotation of  $\psi$  shows that  $u$  and  $v$  do transform as vectors, since

$$R^1R^2(u + Iv)^1\epsilon = (R(u + Iv)\tilde{R})^1\epsilon. \quad (5.24)$$

So, while an antisymmetric  $\psi$  provides a useful way of generating a spin-0 wave equation, the wavefunction clearly contains some spin-1 terms.

The Dirac equation (5.18) applied to the antisymmetric state  $\psi$  leads to a first order version of the Klein–Gordon equation, in a form similar to that first obtained by Kemmer,

$$\begin{aligned} \nabla(\alpha + I\beta) &= m(u + Iv) \\ \nabla(u + Iv) &= -m(\alpha + I\beta). \end{aligned} \quad (5.25)$$

Two degrees of freedom are eliminated by the Dirac equation, which sets  $\theta = \alpha$  and  $\eta = -\beta$ . The equations describe a complex scalar field, with an associated first-order potential of the form of a vector + trivector. The complex structure now arises naturally on the pseudoscalar. The field equations are obtained simply from the standard Dirac Lagrangian, which takes the MSTA form

$$L = \langle \nabla^1\psi(I\gamma_3)^1\tilde{\psi} - m\psi\tilde{\psi} \rangle. \quad (5.26)$$

The canonical stress-energy tensor defined by this Lagrangian is

$$T(a) = \langle a \cdot \nabla^1\psi(I\gamma_3)^1\tilde{\psi} \rangle_1^1 \quad (5.27)$$

where the right-hand side denotes the projection onto the vectors in particle space 1. The surprising feature of this stress-energy tensor is that it is *not* equal to that usually assigned to the Klein–Gordon field. In terms of  $\psi$  the conventional stress-energy tensor is

$$T(a) = m\langle a^2\psi\gamma_0^1\gamma_0^2\tilde{\psi} \rangle_1^1. \quad (5.28)$$

This stress-energy tensor is canonical to a somewhat strange symmetry of the Lagrangian and is not obviously related to translations.

In terms of a complex scalar field  $\phi$  the conventional stress-energy tensor is

$$T(a)_{\text{conv}} = \frac{1}{4}(\nabla\phi a \nabla\phi^* + \nabla\phi^* a \nabla\phi + 2m^2\phi\phi^*), \quad (5.29)$$

whereas our stress-energy tensor is

$$T(a) = \frac{1}{4}(\nabla\phi^* a \cdot \nabla\phi + \nabla\phi a \cdot \nabla\phi^* - \phi^* a \cdot \nabla(\nabla\phi) - \phi a \cdot \nabla(\nabla\phi^*)). \quad (5.30)$$

Both tensors are symmetric and have the same form for plane-wave states. They differ by a total divergence and lead to the same total energy when integrated over a hypersurface. The results of quantum field theory are therefore largely unaffected by the choice of tensor. But gravity is affected by the *local* form of the matter stress-energy tensor, which raises the question; which is the correct stress-energy tensor to use as a source of gravitation? This is a particularly important question to resolve because the stress-energy tensor for the scalar field is a cornerstone of many areas of modern cosmology, including inflation, quintessence, and cosmic strings. The two stress-energy tensors clearly produce different dynamics in a cosmological setting because the conventional tensor includes pressure terms which are absent from our new tensor. Furthermore, the coupling to gravity is different for the two fields, as the antisymmetrised MSTA state couples into the torsion sector of the theory.

### 5.3 Twistors and conformal geometry

In section 4.2 we saw that the orthogonal group  $O(2,4)$  provides a double-cover representation of the spacetime conformal group. The representation is a double cover because the null vectors  $X$  and  $-X$  generate the same point in spacetime. For physical applications we are typically interested in the restricted conformal group. This consists of transformations that preserve orientation and time sense, and contains translations, proper orthochronous rotations, dilations and special conformal transformations. The restricted orthogonal group,  $SO^+(2,4)$ , is a double-cover representation of the restricted conformal group. But the group  $SO^+(2,4)$  itself has a double-cover representation provided by the rotor group  $\text{spin}^+(2,4)$ . So the group of all rotors in conformal space is a four-fold covering of the restricted conformal group. The rotor group  $\text{spin}^+(2,4)$  is isomorphic to the Lie group  $SU(2,2)$ , so the action of the restricted conformal group can be represented in terms of complex linear transformations of four-dimensional vectors in a complex space of signature  $(2,2)$ . This is the basis of the *twistor* programme, initiated by Roger Penrose.

We can establish a simple realisation of a single-particle twistor in the STA. We define the spinor inner product by

$$\langle \tilde{\psi}\phi \rangle_q = \langle \tilde{\psi}\phi \rangle - \langle \tilde{\psi}\phi I\sigma_3 \rangle I\sigma_3. \quad (5.31)$$

This defines a complex space with precisely the required  $(2,2)$  metric. We continue to refer to  $\psi$  and  $\phi$  as *spinors*, as they are acted on by a spin representation of the restricted conformal group. To establish a representation of the conformal group we simply need a representation of the bivector algebra of  $\mathcal{G}(2,4)$  in terms of an action on spinors in the STA. A suitable

representation is provided by [10]

$$\begin{aligned} e\gamma_\mu &\leftrightarrow \gamma_\mu\psi\gamma_0 I\sigma_3 = \gamma_\mu\psi I\gamma_3, \\ \bar{e}\gamma_\mu &\leftrightarrow I\gamma_\mu\psi\gamma_0. \end{aligned} \quad (5.32)$$

One can now track through to establish representations for the action of members of the conformal group. A spacetime translation by the vector  $a$  has the spin representation

$$T_a(\psi) = \psi + a\psi I\gamma_3\frac{1}{2}(1 + \sigma_3). \quad (5.33)$$

It is straightforward to establish that the spinor inner product  $\langle\tilde{\psi}\phi\rangle_q$  is invariant under this product.

If we now pick a spinor  $\phi$  to represent the origin in spacetime, we can write

$$\phi = \zeta\frac{1}{2}(1 + \sigma_3) - \pi I\sigma_2\frac{1}{2}(1 - \sigma_3), \quad (5.34)$$

where  $\zeta$  and  $\pi$  are Pauli spinors. The conventional STA representation of the (valence-1) *twistor*  $Z^\alpha = (\omega^A, \pi_{A'})$  is obtained by applying a translation of  $-r$  [21]

$$Z = \phi - r\phi I\gamma_3\frac{1}{2}(1 + \sigma_3). \quad (5.35)$$

In twistor theory, twistors are viewed as more primitive objects than points, with spacetime points generated by antisymmetrised pairs of twistors. The condition that two twistors generate a real point can be satisfied by setting

$$\begin{aligned} X &= \omega\frac{1}{2}(1 - \sigma_3) + r\omega I\gamma_3\frac{1}{2}(1 + \sigma_3) \\ Z &= \kappa\frac{1}{2}(1 - \sigma_3) + r\kappa I\gamma_3\frac{1}{2}(1 + \sigma_3), \end{aligned} \quad (5.36)$$

where  $\omega$  and  $\kappa$  are Pauli spinors. The antisymmetrised product of  $X$  and  $Z$  can be constructed straightforwardly in the MSTA as

$$\psi_r = (X^1 Z^2 - Z^1 X^2)E. \quad (5.37)$$

If we now apply the decomposition of equation (5.23) we find that

$$\psi_r = (r \cdot r \epsilon - (r^1 \epsilon \gamma_0^1 + r^2 \epsilon \gamma_0^2)J - \bar{\epsilon})\langle I\sigma_2 \tilde{\omega} \kappa \rangle_q. \quad (5.38)$$

The singlet state  $\epsilon$  therefore represents the point at infinity, with  $\bar{\epsilon}$ , representing the origin ( $r = 0$ ). Furthermore, if  $\psi_r$  and  $\phi_s$  are the valence-2 twistors representing the points  $r$  and  $s$ , we find that

$$-\frac{\langle\tilde{\psi}_r\phi_s\rangle_q}{2\langle\tilde{\psi}_r\epsilon\rangle_q\langle\tilde{\phi}_s\epsilon\rangle_q^*} = (r - s) \cdot (r - s). \quad (5.39)$$

The multiparticle inner product therefore recovers the square of the spacetime distance between points. This establishes the final link between the

MSTA, twistor geometry and the conformal representation of distance geometry of equation (4.8). Conformal transformations are applied as joint transformations in both particle spaces. So, for example, a translation is generated by

$$\psi_r \mapsto \psi'_r = T_{a^1} T_{a^2} \psi_r. \quad (5.40)$$

After a little work we establish that

$$\psi'_r = (r+a) \cdot (r+a) \epsilon - (r+a)^1 \eta \gamma_0^1 J - \bar{\epsilon}, \quad (5.41)$$

as required (see also [23]).

We have now established a multiparticle quantum representation of conformal space, so can apply the insights of section 4.2 to extend the representation to de Sitter and anti-de Sitter spaces. We have seen that the *infinity twistor* of Lorentzian spacetime is represented by the singlet state  $\epsilon$ . It follows that the infinity twistors for de Sitter and anti-de Sitter spaces are  $(\epsilon + \bar{\epsilon})$  and  $(\epsilon - \bar{\epsilon})$  respectively [1]. Much work remains in fully elucidating aspects of the twistor programme in the MSTa setup. The links described in this paper should convince the reader that this will prove to be a fruitful line of research. Furthermore, the representation of conformal transformations developed here is naturally related to supersymmetry. This suggests that conformal spacetime algebra may well prove to be the natural setting for supersymmetric field theory.

## Acknowledgements

The work reviewed in this paper has been carried out in collaboration with a number of researchers. In particular, we thank Jonathan Pritchard, Alejandro Cáceres, Rachel Parker, Suguru Furuta and Stephen Gull of the University of Cambridge. As ever, we have benefited enormously from discussions with David Hestenes.

## REFERENCES

- [1] E. Arcaute, A. Lasenby and C. Doran, Twistors and geometric algebra. To be submitted to *J. Math. Phys.*
- [2] V. Bargmann and E. Wigner, Group theoretical discussion of relativistic wave equations, *Proc. Nat. Sci. (USA)* **34**, p. 211 (1948).
- [3] P.A. Collins, R. Delbourgo and R.M. Williams, On the elastic Schwarzschild scattering cross section. *J. Phys. A*, **6**, pp. 161–169 (1973).
- [4] C. Dolby and S. Gull, New approach to quantum field theory for arbitrary observers in electromagnetic backgrounds, *Annals.Phys.*, **293**, pp. 189–214 (2001).
- [5] C.J.L. Doran. *Geometric Algebra and its Application to Mathematical Physics*. Ph.D. thesis, Cambridge University, 1994.

- [6] C.J.L. Doran, A. N. Lasenby and S. F. Gull, States and Operators in the Spacetime Algebra, *Found. Phys.* **23**(9), pp. 1239–1264 (1993).
- [7] C. Doran, A. Lasenby, S. Gull, S. Somaroo and A. Challinor, Spacetime algebra and electron physics. In P. W. Hawkes, editor, *Advances in Imaging and Electron Physics*, Vol. 95, pp. 271–386, 1996 (Academic Press).
- [8] C. Doran, A. Lasenby and J. Lasenby, Conformal Geometry, Euclidean Space and Geometric Algebra. In J. Winkler & M. Niranjana editors, *Uncertainty in Geometric Computations*, pp. 41–58, Kluwer 2002.
- [9] C. Doran and A. Lasenby, Perturbation Theory Calculation of the Black Hole Elastic Scattering Cross Section, *Phys.Rev. D* 66 (2002) 024006.
- [10] C. Doran and A. Lasenby, *Geometric Algebra for Physicists*, Cambridge University Press, 2003.
- [11] C. Doran and A. Lasenby, Physical Applications of Geometric Algebra. Lecture course presented at the University of Cambridge. Course notes available at <http://www.mrao.cam.ac.uk/~clifford/ptIIIcourse/>.
- [12] A.W.M. Dress and T.F. Havel, Distance geometry and geometric algebra, *Found. Phys.* **23**, p. 1357 (1993).
- [13] S. F. Gull, A. N. Lasenby and C. J. L. Doran, Electron Paths, Tunnelling and Diffraction in the Spacetime Algebra, *Found. Phys.* **23**(10), pp. 1329–1356 (1993).
- [14] T. Havel and C. Doran, Geometric algebra in quantum information processing. In S. Lomonaco, ed. *Quantum Computation and Quantum Information Science*, pp. 81–100. AMS Contemporary Math series (2000). quant-ph/0004031
- [15] D. Hestenes, *Space-time Algebra*, Gordon and Breach, 1966.
- [16] D. Hestenes, *New Foundations for Classical Mechanics (Second Edition)*, Kluwer Academic Publishers, Dordrecht, 1999.
- [17] D. Hestenes, Old Wine in New Bottles: A new algebraic framework for computational geometry, <http://modelingnts.la.asu.edu/html/OldWine.html>.
- [18] D. Hestenes and G. Sobczyk, *Clifford algebra to geometric calculus: a unified language for mathematics and physics*, D. Reidel, Dordrecht, 1984.
- [19] T. W. B. Kibble, Lorentz invariance and the gravitational field, *J. Math. Phys.*, **2**(3), p. 212 (1961).
- [20] A. Lasenby, Conformal Geometry and the Universe. To appear in *Phil. Trans. R. Soc. Lond. A*.
- [21] A. Lasenby, C. Doran and S. Gull. 1993. 2-spinors, twistors and supersymmetry in the space-time algebra. In Z. Oziewicz, B. Jancewicz and A. Borowiec, editors, *Spinors, Twistors, Clifford Algebras and Quantum Deformations*, p. 233. Kluwer Academic. Dordrecht.
- [22] A. Lasenby, C. Doran and S. Gull, Gravity, gauge theories and geometric algebra, *Phil. Trans. Roy. Soc. Lond. A* (1998) **356**, pp. 487-582.
- [23] A. Lasenby and J. Lasenby, Applications of geometric algebra in physics and links with engineering. In E. Bayro and G. Sobczyk eds. *Geometric algebra: a geometric approach to computer vision, neural and quantum computing, robotics and engineering*, pp. 430–457. Birkhäuser 2000.

- [24] A. Lasenby and J. Lasenby, Surface evolution and representation using geometric algebra, In Roberto Cipolla and Ralph Martin eds *The Mathematics of Surfaces IX: Proceedings of the ninth IMA conference on the mathematics of surfaces*, pp. 144–168. Springer, London 2001.
- [25] A.N. Lasenby, J. Lasenby and R. Wareham, A covariant approach to geometry and its applications in computer graphics, 2003. Submitted to *ACM Transactions on Graphics*.
- [26] A. Lasenby and C. Doran, Geometric Algebra, Dirac Wavefunctions and Black Holes. In P.G. Bergmann and V. de Sabbata eds., *Advances in the Interplay Between Quantum and Gravity Physics*, Kluwer 2002, pp. 251–283.
- [27] A. Lasenby, C. Doran, J. Pritchard and A. Cáceres, Bound States and Decay Times of Fermions in a Schwarzschild Black Hole Background, gr-qc/0209090.
- [28] H. Li, Hyperbolic Geometry with Clifford Algebra, *Acta Appl. Math.* **48**, pp. 317–358 (1997).
- [29] J. Maldacena, The Large N Limit of Superconformal Field Theories and Supergravity, *Adv. Theor. Math. Phys.*, **2** pp. 231–252 (1998).
- [30] R. Parker and C. Doran, Analysis of 1 and 2 Particle Quantum Systems using Geometric Algebra. In C. Doran, L. Dorst and J. Lasenby eds. *Applied Geometrical Algebras in computer Science and Engineering*, p. 215, AGACSE 2001, Birkhäuser 2001. quant-ph/0106055
- [31] R. Penrose and W. Rindler, *Spinors and Space-time, Volume 1, Two-Spinor Calculus and Relativistic Fields*, (Cambridge University Press 1984).
- [32] R. Penrose and W. Rindler, *Spinors and Space-time, Volume 2, Spinor and Twistor Methods in Space-time Geometry*, (Cambridge University Press 1986).

Anthony Lasenby  
 Astrophysics Group, Cavendish Laboratory  
 Madingley Road, Cambridge, CB3 0HE, UK  
 E-mail: a.n.lasenby@mrao.cam.ac.uk

Chris Doran  
 Astrophysics Group, Cavendish Laboratory  
 Madingley Road, Cambridge, CB3 0HE, UK  
 E-mail: c.doran@mrao.cam.ac.uk

Elsa Arcaute  
 Astrophysics Group, Cavendish Laboratory  
 Madingley Road, Cambridge, CB3 0HE, UK  
 E-mail: ea235@mrao.cam.ac.uk

Submitted: January 16, 2002; Revised: TBA.